

This is the **accepted version** of the journal article:

Tura Poch, Clàudia; Prat Vericat, Maria; Sorbelli, Leonardo; [et al.].
«Late Pleistocene Mediterranean lynx remains from Avenc del Marge del
Moro (NE Iberian Peninsula)». *Historical Biology*, (March 2022). DOI
10.1080/08912963.2022.2043292

This version is available at <https://ddd.uab.cat/record/257224>

under the terms of the  ^{IN} COPYRIGHT license

Late Pleistocene *Lynx pardinus* remains from Avenc del Marge del Moro (NE Iberian Peninsula).

Clàudia Tura-Poch¹, Maria Prat-Vericat¹, Leonardo Sorbelli¹, Isaac Rufi², Alberto Boscaini³, Dawid A. Iurino⁴, Joan Madurell-Malapeira^{1,5,*}

¹Institut Català de Paleontologia, Universitat Autònoma de Barcelona, Cerdanyola del Vallès, 08193. Barcelona. Spain.

²Departament d'Història i Història de l'Art, Universitat de Girona, 17004 Girona, Spain.

³Instituto de Ecología, Genética y Evolución de Buenos Aires (IEGEB – CONICET), DEGE, Facultad de Ciencias Exactas y Naturales, Universidad de Buenos Aires. Int. Guiraldes 2160, Buenos Aires, Argentina.

⁴PaleoFactory, Dipartimento di Scienze della Terra, Sapienza Università di Roma, Piazzale A. Moro 5, 00185 Roma, Italy.

⁵Secció Villalta, Federació Catalana d'Espeleologia, 08025 Barcelona, Spain.

Abstract

During 2011, an international team of scientists successfully obtained for the first-time paleoDNA data from different samples of *Lynx* remains from the Iberian Peninsula. These results showed that these remains belonged to the species *Lynx pardinus* which is, at present, one of the most critically endangered felids. One of the remains sampled in the aforementioned study comes from a small chasm called Avenc del Marge del Moro in the Garraf Massif, with an estimated absolute chronology of 21 ka. Further morphological studies reinforced the last evidence, corroborating the presence of *Lynx pardinus* from the Early to Late Pleistocene in Southern Europe.

Here, we provide for the first time a detailed description of the lynx remains from Avenc del Marge del Moro, which consist of a remarkably complete fossil cranium, as well as several dentognathic and postcranial remains. Our preliminary morphological results, based on cranial specimens, suggest the inclusion of these specimens in the hypodigm of *L. pardinus*.

In the light of the evidence reported the last 10 years for fossil *L. pardinus* and its past distribution throughout southern France and the Iberian and Italian Peninsulas, we further suggest a formal change of the vernacular name of this species to

“Mediterranean lynx”. This also provides novel insight for future reintroduction opportunities of this species alongside the north Mediterranean coast in order to enhance its survival possibilities in wild ecosystems.

Key words: *Lynx pardinus*, Late Pleistocene, Iberian Peninsula, Carnivora, Felidae

*Corresponding author: jmadurell@icp.cat

1. Introduction

The Iberian lynx (*Lynx pardinus*) is currently classified as “endangered” by the IUCN (Rodríguez and Calzada 2015). Today, this threatened species only survives in wild conditions in a few restricted regions of Andalusia (Spain), specifically in the areas of Doñana-Aljarrafe and Sierra Morena (Andújar-Cardena) (Guzmán et al. 2004). *Lynx pardinus* was historically recorded in a larger area of the Iberian Peninsula, but it undertook a biogeographic regression starting from the first decades of the twentieth century, and the decline dramatically increased in the 60’s (Guzmán et al. 2004). The decrease of lagomorph populations, the destruction of their habitats and the high mortality as a consequence of human activity are among the main factors which influenced in the extinction of lynx in most of its historical range (Guzmán et al. 2004). For these reasons, in 2002 the Iberian lynx was classified as a critically endangered species by the IUCN (Rodríguez and Calzada 2015). However, in 2015 this species shifted to a lower degree of threat in the Red List of endangered species of the IUCN (Rodríguez and Calzada 2015). This was possible thanks to the repopulation of some individuals in Guadalmellato and Guarrizas around 2010 (Simón 2013).

The origin of the genus *Lynx* is still largely unknown, but there is a certain consensus in identifying the Pliocene to Early Pleistocene species *Lynx issiodorensis* as the ancestor of all extant *Lynx* species (Werdelin 1981). *L. issiodorensis* earliest records corresponds to the European Early Pliocene (ca. 4.0Ma) being widely distributed through the Northern Hemisphere in the Middle Villafranchian (Werdelin 1981; Boscaini et al. 2015). The Eurasian fossil record evidence that *L. issiodorensis* first appeared in the Late Pliocene later becoming widely distributed in Eurasia by the Early Pleistocene (ca. 2.6 Ma; Boscaini et al. 2015). The first probable speciation process from this putative common ancestor took place around 2.4-2.5 Ma in North America, with the split of *L. rufus*. *Lynx lynx* appears in Asia at the end of Early Pleistocene, subsequently spreading throughout Europe at the Pleistocene-Holocene transition. Around the same time, a population of *L. lynx* entered in North America, where the speciation to *L. canadiensis* took place and consequently *L. rufus* was displaced into more southern geographic areas (Werdelin 1981).

In southern Europe, Boule and Villeneuve (1927) attributed the Late Pleistocene cranial remains of Grotte de l'Observatoire (Monaco) to *Felis (Lynx) pardina*, race *spelaea*, considering it as an intermediate form between *L. lynx* and *L. pardinus*. Subsequently, Werdelin (1981) described an anagenetic lineage from *L. issiodorensis* to *L. pardinus pardinus*, with *L. i. valdarensis* and *L. p. spelaeus* as intermediate forms, characterized by the decrease in size and a relative lengthening of the first lower molar. This author also suggested that this decrease in size could be a response to the competition with other European carnivores, like *Panthera schaubi* (*Puma pardoides*), which led lynxes to prey on smaller animals. It's important to remark that the split of *L. pardinus* from *L. issiodorensis* during this faunal transition coincides

with the speciation of *Oryctolagus lacosti* and *Oryctolagus layensis* from about 2 Ma (Boscaini et al. 2015). Although *O. layensis* was only present in the Iberian Peninsula, *O. lacosti* is also found in the fossil record of southern France (Biju-Duval et al. 1991).

During the twentieth century, several authors considered *L. pardinus* as a local variety of the European *L. lynx* (for a review see Wilson and Reeder 2005, Boscaini et al. 2016). However, subsequent morphological (Werdelin 1981; Garcia-Perea et al. 1985) and genetic (Beltrán et al. 1996; Johnson et al. 2004) studies concluded that *L. pardinus* and *L. lynx* are distinct species, that independently diverged from *L. issiodorensis*. Garcia-Perea et al. (1985) analysed different cranial remains of *L. pardinus* and *L. lynx* and concluded that the skulls of *L. pardinus* display a high degree of homogeneity, with only reduced variability between males and females. The skull of *L. pardinus* appears smaller and with a more prominent interorbital convexity, if compared to that of *L. lynx* (Garcia-Perea et al. 1985). Also, *L. pardinus* has a remarkably shorter sagittal crest than *L. lynx*, a feature that is probably related to the general smaller size of the preys of the Iberian lynx (Garcia-Perea et al. 1996).

To date, the earliest remains of *L. pardinus* are those recovered in the Avenc Marcel cave with an inferred absolute chronology of 1.7 Ma. Recent DNA analyses estimated that the Iberian lynx lineage originated around 1.53–1.68 Ma (Johnson et al. 2004; See Li et al. 2016 for alternative views), placing the remains from Avenc Marcel chronologically close to the purported origin of the species. This speciation event was probably influenced by the glacial pulse at 1.8 Ma, roughly coinciding with the Middle-Late Villafranchian boundary (Boscaini et al. 2015). The climate change induced the faunal reorganization of the beginning of the Late Villafranchian, which imply the extinction of several Middle Villafranchian taxa, and its replacement by new incoming

taxa, especially from Asia. While herbivores migrated and/or adapted according to the environmental conditions, their predators moved after them, so new carnivorans dispersed into Europe, like *Pachycrocuta brevirostris* (Iannucci et al. 2021) and *Panthera gombaszoegensis* (Palombo et al. 2008).

Boscaini et al. (2016) considered *L. spelaeus* and *L. pardinus spelaeus* as junior synonyms of *L. pardinus*. This species was widely distributed across the Mediterranean area since the late Early Pleistocene being subsequently recorded during the Middle and Late Pleistocene in France and Italy (Ghezzo et al. 2014; Boscaini et al. 2016). In a recent review of fossil lynxes from southwestern Europe, Mecozzi et al. (2021) reported the presence of *L. pardinus* also at southern latitudes of the Italian Peninsula during the Late Pleistocene.

In the present work, we describe previously unpublished dentognathic and postcranial remains of Late Pleistocene Iberian lynx from the Avenc del Marge del Moro (northeastern Iberian Peninsula). These remains are compared with other lynx remains of extant and extinct species, in order to properly characterize the morphology of this fossil sample. This material attests for the continuous presence of this felid in the Iberian Peninsula since the Early Pleistocene, allowing to illuminate the evolutionary history of this species.

2. Geological and geographical background

Avenc del Marge del Moro (41°21'33''N and 5°37'19''E) is located at an altitude of 480 m above the sea level, and in proximity of the limit between the villages of Vallirana and Begues (Baix Llobregat, Catalonia; Fig. 1). The cave is part of an extensive karst complex, mostly located in Pla del Marge del Moro, and is mainly constituted by

calcareous-dolomitic materials from the Triassic Muschelkalk. Avenc del Marge del Moro is close to the main cave of the system, Avenc Marcel (Asensio 1993; Ferro et al. 1998; Blasco et al. 1999; Boscaini et al. 2015).

Avenc del Marge del Moro was first explored in 1924 by Rafael Amat i Carreras accompanied by some Mas de les Fonts residents, during the construction of a high voltage tower. Posteriorly, the main cavity, Avenc Marcel, was discovered in 1982, during the construction of another high voltage tower. In 1990, the exploration works were resumed in order to search new cavities to find an access to Avenc Marcel. In this opportunity Avenc del Marge del Moro was explored in detail and some *Lynx pardinus* remains were found (Asensio 1993; Ferro et al. 1997; 1998). In 1995, the first archaeological survey was performed and allowed to recover a Neolithic burial. Afterwards, an Epipaleolithic assemblage was excavated, during 1997-1998 (Blasco et al. 1999).

The layers of Avenc del Marge del Moro reveal an archeological assemblage, which denotes the human exploitation of the cave during Neolithic and Epipaleolithic age (Blasco et al. 1999). Regarding the paleontological remains, the following species have been identified at Avenc del Marge del Moro: *Sciurus vulgaris*, *Eliomys quercinus*, *Oryctolagus cuniculus*, *Crocidura russula*, *Meles meles*, *Canis lupus*, *Felis sylvestris* and *Lynx pardinus*. They have been recovered on the surface of the galleries and buried into silty sediment, in a chaotic distribution as a result of the action of the runoff water. The important accumulation of *O. cuniculus* remains revealed a relevant number of bite-marks, which were related to *L. pardinus* activity (Ferro et al. 1997). Also, AMS ¹⁴C analyses allowed to determine an absolute age of 20.551–21.413 cal ka BP for the fossil assemblage (Rodríguez et al. 2011).

3. Materials and methods

This work presents *Lynx pardinus* remains from Avenc del Marge del Moro, which are housed in the Institut Català de Paleontologia Miquel Crusafont (Sabadell, Spain). These fossils were discovered in the 90's during fieldwork activities, in "recollection points" A, B, D, E (Ferro et al. 1997; Fig. 1). They were collected on the surface and within the deposits of clay sediment. This irregular deposition due to water activity also impeded to observe horizontal stratigraphy (Ferro et al. 1997). The Avenc del Marge del Moro remains were described by Ferrero et al. (1997) and attributed to both *L. pardinus* and *L. spelaea*, but Boscaini (2014) preliminarily assigned all of them to *L. pardinus*.

To describe and compare the craniodental remains of *L. pardinus*, we focused on the diagnostic features of this species remarked by Garcia-Perea et al. (1985), Boscaini et al. (2015; 2016) and Mecozzi et al. (2021). Measurements of the studied specimens were taken with a calliper to the nearest 0.1 mm. Measurements from Viret (1954), Bonifay (1971), Clot and Besson (1974), Kurtén (1978), Altuna (1980), Clot (1988), Ginsburg (1998), Testu (2006), Castaños et al. (2009), Cipullo (2010) and Ghezzi et al. (2015) were taken into account for biometric comparisons. The results presented by Boscaini et al. (2015; 2016) and Mecozzi et al. (2021) have been used to conduct morphological comparisons. Moreover, skulls and postcranial material of extant *L. lynx* (2010-1402; 2010-1403), *L. rufus* (IPS 82317), *L. canadensis* (IPS 82318) and *Caracal caracal* (IPS 82319) have also been used for morphological comparisons.

Anatomical abbreviations—I3: third upper incisive; C1: first upper canine; P3: third upper premolar; P4: fourth upper premolar; c1: first lower canine; p3: third lower premolar; p4: fourth lower premolar; m1: first lower molar; Mtc: metacarpus; Mtt:

metatarsus; L: mesiodistal length; W: buccolingual width; H: height; Lpr: protocone mesiodistal length; Lps: parastyle mesiodistal length; Lpa: paracone mesiodistal length; mesastyle mesiodistal length; GL: greatest proximodistal length; DT prox.: proximal epiphysis mediolateral diameter; DAP prox.: proximal epiphysis anteroposterior diameter; DT diaf.: diaphysis mediolateral diameter; DAP diaf.: diaphysis anteroposterior diameter; DT dist.: distal epiphysis mediolateral diameter; DAP dist.: distal epiphysis anteroposterior diameter; BPacr: greatest breadth across the *processus articularis*; HFcr: greatest height of the *facies terminalis cranialis*; BFcr: greatest breadth of the *facies terminalis cranialis*; Bpacd: greatest breadth across the *processus articularis caudalis*; PL: physiological length of the body; LA: length of the acetabulum including the lip; SH: smallest height of the shaft of ilium; SB: smallest breadth of the shaft of ilium; LFo: inner length of the foramen *obturatum*; HS: height along the spine; SLC: smallest length of the *collum scapulae*; GLP: greatest length of the *processus articularis*; LG: length of the glenoid cavity; BG: breadth of the glenoid cavity.

Institutional abbreviations—ICP: Institut Català de Paleontologia Miquel Crusafont; IPS, acronym of the collections of Institut Català de Paleontologia Miquel Crusafont; IUCN: International Union for Conservation of Nature.

4. Results

4.1 Referred specimens—Supplementary material

4.1. Measurements—Tables 1, 2, 3 and 4

4.2. Description

4.2.1. *Craniodental specimens*

Cranium — IPS4175 shows most of the splanchnocranium and only the zygomatic and nasal bones are missing, whereas IPS4176 consists of a well preserved neurocranium (Figs. 2, 3, S1). Overall, the crania are anteroposteriorly elongated with a domed profile in lateral view (Figs. 2, 3, S1). In dorsal view, the temporal ridges of both specimens are long and parallel to each other, forming a lyre-shaped surface on the cranial roof (Figs. 2, 3, S1A1-B1). This results in a short sagittal crest, which originates anteriorly at the junction of the temporal lines and merges posteriorly with the nuchal crest (Figs. 2, 3). In IPS4175 (Figs. 2, S1A1-A4) the posterior sutural contacts are more separated than those on the other specimens, suggesting a sub-adult condition of this individual. The tympanic bullae are prominent, elliptic in shape and elongated anteromedially to posterolaterally. The jugular and hypoglossal foramina are confluent in the same cavity in both the specimens (Fig. 2, S1A4, B4). In IPS4176, the insertions of the parietoscutular muscle, the cervicoscutular muscle and the occipital muscle are well marked, drawing a more distinguishable sulcation between the nuchal crest and the sagittal crest than in IPS4175 (Figs. 2, 3, S1A1, B1). In ventral view, the occipital bone shows a shallow sulcus surrounding the tympanic bulla medially and posteriorly, near the insertion of the *musculus rectus capitis ventralis*. The foramen magnum is oval and slightly compressed dorsoventrally.

Garcia-Perea (1998) distinguished three types of maxillopalatine sutures. Among them, type 1 is characterized by a straight boundary between the horizontal palatine plates and the choanae, with a small triangular groove in the centre. This morphology is the most common since it is observed in the 86% of the sample of *L. pardinus* analysed by Garcia-Perea (1998) and is also observed in the lynx remains from Avenc del Marge del Moro (IPS4175; Fig. 2, S1A4, B4).

Upper Dentition—The upper canines are only partially preserved in IPS4242 (Fig. S2D). They are robust and mesiodistally compressed, and in buccal view they show the double sulcation that is typical of the genus *Lynx*.

The upper molars and premolars are preserved in the cranium IPS4175 (Figs. 2,3, S1A), the right maxilla IPS4177 and the left maxilla IPS41789. The two latter remains and the cranium IPS4176 probably correspond to the same individual (Fig. 2, S1B). In addition, IPS4181 and IPS4179 still preserve the left P3 (Fig. S2A) and the left P4 (Fig. S2D), respectively. The P3 is buccolingually compressed, with the cusps mesiodistally aligned. The paracone is the highest cusp, whereas the parastyle is absent. The metastyle is smaller than the paracone and presents a small distal cingulum. The P4s display small and round protocones located lingually, between the parastyle and paracone. The P4 parastyle, paracone and metastyle are buccolingually compressed. Also, in all the available P4s, the ectoparastyle is absent (Figs. 2, 3, S1A-B).

Lower Dentition—The lower canines display a conic shape (Fig. S2E-G). IPS4221 presents a double sulcation in anterior view, whereas, in IPS4222, these sulci are more medially situated. The p3 (IPS4180; Fig. S2C) is buccolingually compressed and the paraconid is well-distinguishable. In the distal side of the hypoconid there is a well-developed cingulum.

4.2.2. *Postcranial remains*

Scapula— An almost complete right scapula (IPS4233), only lacking part from the infraspinatus fossa and a fragment of the supraspinatus fossa was recovered. Also, three left distal fragments (IPS4243, IPS4244, IPS4232), and one right proximal fragment (IPS4231) are available. All glenoid cavities display a drop-like shape in

anterior view. The triceps insertion in IPS4232, IPS4231 and IPS4243 are very well-marked, especially in IPS4232 (Fig. 4B, E).

Humerus—There are only two humeral fragments in the sample (Fig. 4A, C): a distal epiphysis lacking the lateral epicondyle (IPS4215) and one distal portion of humerus (IPS4201). Both remains display a well-developed olecranon fossa. IPS4201 is overall slender when compared with IPS4125, and its epicondylar crest is broader anteroposteriorly. In addition, IPS4201 presents an elongated supracondylar foramen, as is typical for Felidae (Fosse et al., 2020).

Radius—Three proximal fragments of radii are available for observations (Fig. 4D, G). Two of them are right-sided (IPS4193 and IPS4198) and one is left-sided (IPS4197). The radial tuberosity is well-marked, especially in IPS4193 and IPS4197. The proximal epiphysis is elliptical and anteroposteriorly compressed in proximal view.

Ulna—The almost complete left ulna only lacks the distal epiphysis (IPS 4202; Fig. 4H). The olecranon displays a central depression, delimited by a bulge situated in caudal position and another located in proximomedial position. The caudal edge is projected from the medial surface below the trochlear notch. In distal view, the upper border of the olecranon is well-detached.

Metacarpals— A third left metacarpal (IPS4218) (Fig. 4F) shows an overall slender morphology with a slight palmar curvature. The insertion for the *flexor carpi radialis* muscle is well marked.

Pelvis—The three available hemipelvis remains belong to the left side (Fig. 5G) and only IPS4211 is complete. On the contrary, IPS4210 lacks the pubic portion and IPS4207 only consists of three ilium fragments. In all these remains (excluding IPS4207), the iliac

tuberosity is only barely distinguishable, the general morphology is indistinguishable from other members of the *Lynx* genus.

Femur—The left femur distal epiphysis (IPS 4214) belongs to a juvenile individual (Fig. 5H) with complete epicondyles.

Tibia—Two of the recovered tibiae are complete, only lacking the proximal epiphyses, which are not completely fused (IPS4212 and IPS4213; Fig. 5E, F), thereby suggesting they belong to juvenile individuals. A third tibial remain is only constituted by a fragment of diaphysis (IPS4226). IPS4212 and IPS4213 show a straight and slender diaphysis with only slightly marked muscular insertions in the posteroproximal part.

Metatarsals—Two 2nd metatarsals (IPS4219; IPS4194), a 3rd metatarsal (IPS4216), and a 5th metatarsal (IPS4220) are available (Fig. 5 A-D). Like the metacarpals, also the metatarsals display a slender and straight diaphysis, showing also a marked palmar curvature.

5. Discussion

5.1. Comparisons with extant and fossil lynx species

5.1.1. Cranial comparisons

Cranial remains of extant and extinct *L. pardinus* are mainly characterised by a postorbital constriction that is wider than in *L. lynx*, long and parallel temporal ridges, and the confluence of the jugular and hypoglossal foramina. In the dentition, the P4 usually lacks the ectoparastyle, and the m1 metaconid is generally absent or extremely reduced (Boule and Villeneuve 1927; Garcia-Perea 1985; 1996; Boscaini et al. 2015; 2016; Mecozzi et al. 2021).

In dorsal view, the cranial remains from Avenc del Marge del Moro display short sagittal crests and long temporal ridges in comparison to *L. lynx*, being similar to the morphology observed in extant *L. pardinus*. The crania of fossil and extant Iberian lynxes are similar to those of *L. canadensis* and *L. rufus* in this aspect, which also display a short sagittal crest and well-developed lyre-shaped temporal ridges (Garcia-Perea 1985; Boscaini 2014).

As stated above, the confluence in the same cavity of the jugular and hypoglossal foramina is observed in the sample from Avenc del Marge del Moro, except for the foramina on the right side of IPS4175, in which the unclear position of the foramina is probably attributable to interspecific variability (Figs. 2, S1). A similar arrangement of the foramina is detectable in *C. caracal*, *L. rufus*, and *L. issiodorensis* s.l. (Fig. 6G-L; Mecozzi et al. 2021). On the other side, *L. lynx* and *L. canadensis* show a more marked septum between the two foramina (Fig. 6; Boscaini 2014).

The braincase of the Iberian lynx is more rounded compared to *L. lynx*, and this feature could be related to a pedomorphic change of shape, also reflected in the conformation of the temporal ridges and the sagittal crest (Garcia-Perea 1996). Such morphology is also displayed by *L. canadensis* (C.T. pers. observ.).

In IPS4176 the presphenoid bone is partially broken, while in IPS4175 it shows a pentagonal shape as noticeable in fossil and extant *L. pardinus* (IPS82320; Fig. 6). In comparison, the presphenoid of *L. rufus* is more anteroposteriorly elongated and culminates in an anteriorly pointed tip. On the contrary, the presphenoid of *L. canadensis* is more medially wider (Huynh et al., 2019), similarly to the *L. pardinus* presphenoid shape, but with a mediolateral constriction approximately in its midshaft (Fig. 6I-K). Concerning *L. lynx*, extant individuals show stronger variation in their

presphenoid morphology, with elongated shapes like *L. rufus*, or pentagonal such as that of *L. pardinus*. In *L. issiodorensis*, the presphenoid morphology is observable in some remains from Olivola (Italy) and Saint-Vallier (France) and appears as wider and rhomboidal-elliptical in shape (Fig. 6).

In *L. pardinus*, the shallow depression surrounding posteromedially the tympanic bulla is less marked than in *L. lynx* and *L. rufus*. Furthermore, the muscular insertions for the *semispinalis capitis*, brachiocephalic and sternocephalic muscles situated ventral to the nuchal crest, are less marked than in *L. lynx*. The insertion of the muscle temporalis is well-developed in *L. issiodorensis* and *L. lynx* and consistently less developed in all the other living species. Nonetheless, the insertions of parietoscutular muscle, cervicoscutular muscle, and occipital muscle are well marked in IPS4176. As a consequence, this muscle insertion area is well defined, and is similar to the conformation observed in extant specimens of *L. pardinus* and *L. lynx*.

5.1.2. Dental comparisons

All the studied P3s show a well-developed paracone, a small metastyle, and a detached distal cingulum. All the analysed P4s from Avenc del Marge del Moro lack the ectoparastyle, as in the extant *L. pardinus* (Kurtén 1978; Boscaini et al. 2016; Mecozzi et al. 2021). The ectoparastyle is usually present in the P4 of *L. lynx* and in the 45% of *L. issiodorensis*. Additionally, according to Mecozzi et al. (2021), the P4 ectoparastyle is mostly always present in *L. lynx* and normally absent in fossil *L. pardinus* being only present in the 13% of the Ingarano sample.

On the morphometric ground, extant *L. pardinus* shows a P4 that is mesiodistally shorter than Pleistocene *L. lynx* and *L. issiodorensis*. Analogously, Late Pleistocene *L.*

issiodorensis specimens from the Italian Peninsula also present a P4 mesiodistal length that is lower than that of earlier *L. issiodorensis* specimens, as already stressed by Werdelin (1981). Consequently, Early Pleistocene P4 lengths of *L. issiodorensis* and *L. pardinus* are very similar in size. These Early Pleistocene *L. issiodorensis* remains from Olivola, Pantalla and Upper Valdarno have been traditionally attributed to *L. issiodorensis valdarnensis*, and considered as representing an intermediate form between *L. issiodorensis* and *L. pardinus* (Werdelin 1981; Cipullo 2010; Cherin et al. 2013). However, Mecozzi et al. (2021) questioned the validity of this subspecies erected on the basis of dental measurements. Regarding *L. pardinus* remains, the P4 size from Avenc del Marge del Moro is in accordance with other coeval remains from the Iberian and Italian Peninsulas, which are altogether smaller than those of Late Pleistocene *L. pardinus* from French sites (Fig. 7). This suggests the presence of a latitudinal size gradient in different *L. pardinus* populations.

5.1.3. Postcranial comparisons

The humeral measurements of the lynx from Avenc del Marge del Moro are included within the range of extant *L. pardinus*. In fact, in the extant Iberian lynx the average value of the distal epiphysis mediolateral diameter (DT dist) is 28.24 mm, with a range of variation comprised between 27.5 and 29.25 mm (Castaños et al. 2009). In IPS4215, DT dist is 29.3 mm, thus reaching the largest value of the *L. pardinus* range. On the contrary, the humerus of extant *L. lynx*, presents consistently larger measurements than *L. pardinus*, with a range of variation comprised between 27.3 to 40.9 and an average of DT dist of 37.1 mm. The general morphology of the humeral distal fragments of Avenc del Marge del Moro does not present significant differences with that of *L. lynx*.

The olecranon fossa is well developed in both remains from Avenc del Marge del Moro, as well as in *L. lynx*. The epicondylar crest in IPS4201 is also well-developed, as in *L. lynx*, but the muscular insertion of the anconaeus muscle is more strongly marked in *L. lynx*, probably related with its larger general size.

Extant and extinct lynx species do not differ considerably on the basis of their radius measurements, in comparison to other postcranial elements (Table 5). However, as was expected, the smallest measurements belong to extant *L. pardinus*, and the largest ones are recorded for extant *L. lynx* and fossil specimens of *L. pardinus* from France. Oblique carpal extensor muscle insertion is slightly visible in IPS4197, and absent in IPS4198, whereas it is greatly developed in *L. lynx*.

The proximal ulnar epiphysis from Avenc del Marge del Moro also evidences that *L. pardinus* from the Pleistocene of France and extant Eurasian lynx have a larger size than extant and extinct *L. pardinus* from the Iberian Peninsula (see in Table 5). Accordingly, the olecranon tuberosity is less prominent in IPS4202 than in *L. lynx*. Moreover, above the anconeal process, *L. lynx* presents a tuberosity related to the muscular insertion of anconeus, which is only slightly marked in the specimen from Avenc del Marge del Moro.

There are no relevant morphological differences between the third metacarpal from Avenc del Marge del Moro and that of *L. lynx*, although metacarpals of *L. pardinus* appear as overall smaller and slender than those of *L. lynx*. As metacarpals, the metatarsal remains of *L. pardinus* do not present visible morphological differences with *L. lynx*. Nevertheless, there is a small difference in the dorsal part of the proximal diaphysis of the fifth metatarsus, with a slight sulcation observable in *L. lynx* and absent in the specimen from Avenc del Marge del Moro.

5.2. Taxonomical considerations

The morphology of the dorsal view of the neurocranium presents the most striking difference between *Lynx pardinus*, *Lynx issiodorensis* and *Lynx lynx*. While *L. issiodorensis* and adult individuals of *L. lynx* displays a long sagittal crest, whereas juvenile and adult *L. pardinus* invariably show well-marked temporal ridges and short sagittal crest (García-Perea 1996; Boscaini et al. 2015). The position of jugular and hypoglossal foramina also allows to distinguish *Lynx pardinus* from *Lynx lynx*. In *L. pardinus* these foramina coalesce in the same cavity as well as in its putative ancestor, *L. issiodorensis* (Mecozzi et al. 2021), whereas *L. lynx* presents a marked septum between them. Regarding the presphenoid, *Lynx rufus* and *Lynx canadensis* present peculiar presphenoid shapes, being respectively narrow and enlarged mediolaterally (Huynh et al. 2019). Also the presphenoid of *Lynx pardinus* is distinguishable, and is characterised by a roughly pentagonal shape. On the contrary, *Lynx lynx* shows different morphologies in this bone, displaying pentagonal, rectangular, and rhomboidal shapes. In *Lynx issiodorensis*, the presphenoid is wide and with an elliptical-rhomboidal shape.

As it has been pointed out by Kurtén (1978), the presence of an ectoparastyle in P4 is a typical feature of *Lynx lynx* and *Lynx issiodorensis*. However, in *Lynx pardinus* the ectoparastyle tends to be absent or poorly developed. In the *L. pardinus* sample from the latest Early Pleistocene site of Vallparadís Estació and Cueva Victoria analysed by Boscaini et al. (2016), only three of nine studied P4 present ectoparastyle. In Middle and Late Pleistocene *Lynx pardinus*, the P4 ectoparastyle could be recorded with even lower percentages (Mecozzi et al. 2021). Accordingly, any of the three P4 found in Avenc del Marge del Moro present the ectoparastyle, coinciding with the results of

Mecozzi et al. (2021), which indicate that 100% of P4 in extant *Lynx pardinus* do not present this feature.

To sum up, the above reported morphological criteria enables us include the studied Late Pleistocene felid remains from Avenc del Marge del Moro to the species *Lynx pardinus* in its wide sense (sensu Boscaini et al. 2016; Mecozzi et al. 2021). Also, it is important to remark that previous DNA studies on the same specimens arrived to the same conclusions (Rodríguez et al. 2011).

As suggested by Werdelin (1981), the P4 mesiodistal length allow to observe the progressive decrease in size in *Lynx pardinus* lineage. Some authors distinguished the subspecies *Lynx pardinus pardinus* and *Lynx pardinus spelaeus*, on the basis of the difference in size (Sarrión 1976; Estévez 1979; Kurtén and Granqvist 1987; Werdelin, 1981; Cardoso 1993; Cipullo 2010; Fosse et al. 2020). Boscaini et al. (2016) attributed this size difference to intraspecific variation because there is no solid morphological basis for distinguishing *L. pardinus* and *L. spelaeus* at a specific or subspecific level. Similar conclusions were reached by Rodríguez-Varela et al. (2015) who realized molecular analyses on several lynx fossil samples and reassigned to *L. pardinus* some specimens from the Late Pleistocene of northern Italy that were previously ascribed to *L. cf. spelaeus* on the basis of their large size. Size differences among *L. pardinus* populations are indeed observable between the smaller forms of the Italian and Iberian Peninsulas and the larger specimens from continental Europe (Fig. 7). From a preliminary standpoint, these size differences could be ascribable to regional ecological variables possibly driven by a latitudinal gradient. Similar intraspecific body size variations have been observed in other carnivorans, like the spotted hyaena (Kurtén 1957). Late Pleistocene lynx remains from Furninha and Casa da Moura (Portugal) were

also ascribed to *Lynx pardinus spelaeus* on the basis of their robustness (Cardoso 1993) and their attribution should be reevaluated in the light of the new evidence. In fact, the average value of their P4s mesiodistal lengths are in accordance with the rest of Late Pleistocene remains from the Iberian Peninsula and differ from those recovered in France, supporting the idea of the presence of a latitudinal-related influence on size.

5.3. Paleobiogeographic implications

The origin of *L. pardinus* probably occurred in the Iberian Peninsula around 1.8 Ma, after the intense glacial stages 66/64, when local populations of *L. issiodorensis* could have remained isolated from the rest of the European continent (Boscaini et al. 2015, 2016). In the Early Pleistocene, *L. pardinus* spread in the Iberian Peninsula and, at the Early-Middle Pleistocene transition started its dispersal towards southern France and northern Italy being finally recorded at Ingarano (southern Italy) at the end of the Late Pleistocene (ca. 0.4 Ma; Mecozzi et al. 2021). In this context, the sample from the Avenc del Margo del Moro, represents the only Late Pleistocene lynx sample from the Iberian Peninsula with reasonably complete cranial and postcranial remains, allowing for a solid attribution to *L. pardinus*. Moreover, from a morphometric standpoint, this sample is similar to that recovered in the Late Pleistocene site of Ingarano. This data attests to the presence of a large and stable population of *L. pardinus* throughout the Mediterranean area during the Late Pleistocene. According to the former assertions and taking into account the northern circum-Mediterranean paleobiogeographic distribution of *L. pardinus* during the Pleistocene, we suggest that a more appropriate vernacular name of this species could be “Mediterranean lynx”. This name, in fact, takes into account the past distribution of this species, in contraposition to “Iberian lynx” which only makes

reference to its current biogeographic range. This is also in line with the name of the other lynx species from Europe, *L. lynx*, whose vernacular name (Eurasian lynx) reflects its past and present distribution.

Despite the considerable number of efforts conducted in the last years to preserve stable populations of *Lynx pardinus* in southern Iberian Peninsula (Guzmán et al. 2004; Rodríguez and Calzada 2015) no previous studies considered the paleobiogeography of this species and the putative viability of their reintroduction in other areas of the Iberian Peninsula or other Mediterranean regions of southern Europe. The above-mentioned data have important consequences for the future conservative efforts with the aim of preserving the variability of *L. pardinus* and open to the possibility of reintroducing stable populations of this species also in northern portion of the Iberian Peninsula, southern France and Italy. In fact, these areas of Mediterranean Europe still present the heterogeneous environments preferred by *L. pardinus* as open mixed grasslands with dens shrubs as junipers or oaks (see the LIFE program and Europe grasslands), allowing for new *L. pardinus* survival opportunities. Furthermore, the main prey of *L. pardinus*, the European rabbit (*O. cuniculus*), was historically reintroduced in some Mediterranean areas such as southern France and central Italy, as well as in Eastern Europe, in the same habitat preferred by *L. pardinus* (Devillard et al., 2008; Santilli and Bagliacca 2010).

Conclusions

The evidence reported here attests for the first time the unquestionable presence of *L. pardinus* in the Late Pleistocene of the northeastern Iberian Peninsula. Previous analyses allowed to recognize the origin of this species in the Early Pleistocene of the

Iberian Peninsula and its expansion throughout the Middle and Late Pleistocene of southern France and Italy. The present data confirms the existence of a circum-Mediterranean stable and uniform population of *L. pardinus* through the Late Pleistocene considerably enlarging the paleogeography of this species and providing promising information for future reintroduction and conservation programs. According to the former data, we suggest to change the common name this species to Mediterranean Lynx.

Acknowledgments

This work was funded by the Agencia Estatal de Investigación-European Regional Development Fund of the European Union (CGL2017-82654-P, AEI/FEDER-UE) and the Generalitat de Catalunya (CERCA Program). J.M.-M. is member of the consolidated research group 2017 SGR 116 (AGAUR, Generalitat de Catalunya). The collaboration of the Catalan Federation of Speleology is acknowledged. J.M.-M. dedicate this work to his friend and mentor Miquel Nebot Obon for his indefectible work and efforts preserving the paleontological heritage in karstic environments.

References

Altuna J. 1980. Hallazgo de un Lince Nórdico (*Lynx Lynx* L. *Mammalia*) en la Sima de Pagolusieta, Gorbea (Vizcaya). *Munibe* 3-4: 317–322.

Asensio T. 1993. Cavidades del pla del Marge del Moro. Nuevos descubrimientos en el Avenc Marçel. *Passamà* 1:27–42.

Blasco A, Mangado X, Villalba MJ., Edo M. 1999. Coveta del Marge del Moro (Bagues. Baix Llobregat). Memòria d'intervenció arqueològica. Generalitat de Catalunya.

Bonifay MF. 1971. Carnivores quaternaires du Sud-Est de la France. Paris: Editions du Muséum Nationale d'Histoire Naturelle.

Boscaini A. 2014. Plio-Pleistocene lynxes (*Lynx ssp.*) from the Iberian Peninsula. Taxonomy and phylogenetic relationships with the extant and fossil species. Master thesis. Barcelona: Universitat Autònoma de Barcelona.

Boscaini A, Madurell-Malapeira J., Llenas M., Martínez-Navarro B. 2015. The origin of the critically endangered Iberian lynx: Speciation, diet and adaptive changes. *Quat Sci Rev.* 123: 247–253.

Boscaini A, Alba DM, Beltrán JF, Moyà-Solà S, Madurell-Malapeira J. 2016. Latest Early Pleistocene remains of *Lynx pardinus* (Carnivora, Felidae) from the Iberian Peninsula: Taxonomy and evolutionary implications. *Quat Sci Rev.* 143: 96–106.

Boule M, Villeneuve L. 1927. La Grotte de l'Observatoire a Monaco. Paris: Massone et Cie Éditeurs.

Biju-Duval C, Ennafaa H, Dennebouy N, Monnerot M, Mignotte F, Soriguer R, El Gaaïed A., El Hili A, Mounolou J.C. 1991. Mitochondrial DNA evolution in *Lagomorpha*: Origin of systematic heteroplasmy and organization of diversity in European rabbits. *Jour Mol Evol.* 33: 92–102.

Cardoso J L. 1993. Contribução para o conhecimento dos grandes mamíferos do Pleistocénico Superior de Portugal. Oeiras: Câmara municipal de Eoeriras.

Castaños P. 1993. Estudio de los macromamíferos de los niveles paleolíticos de Chaves. *Bolskan* 10: 9–30.

Castaños P, Murelaga X, Bailon S, Castaños J, Saez de Lafuente X, Suarez O. 2009. Estudio de los vertebrados del Yacimiento de Lezikako Koba (Kortezubi, Bizkaia). *Kobie* 28: 25–50.

- Cherin M, Iurino DA, Sardella R. 2013. New well-preserved material of *Lynx issiodorensis valdarnensis*. Boll. Soc. Paleo. Ital 52: 103–111.
- Chezzo E, Boscaini A, Madurell-Malapeira J, Rook L. 2015. Lynx remains from the Pleistocene of Valdemino cave (Savona, Northwestern Italy), and the oldest occurrence of *Lynx spelaeus* (Carnivora, Felidae). Rend. Lincei 26: 87–95.
- Cipullo A. 2010. L'evoluzione del genere Lynx dal pliocene al pleistocene medio nell'area mediterranea. Italy: Università degli Studi di Modena e Reggio Emilia.
- Clot A. 1988. Faune Magdalénienne de la Grande Grotte de Labastide (Hautes-Pyrénées, France). Munibe 40: 21–44.
- Clot A, Besson JP. 1974. Nouveaux restes osseux de lynx dans les Pyrenees. Bul Soc Hist Nat Toul. 157–169.
- Daura J, Borràs MS. 2009. Historiografia dels jaciments plistocens al massís del Garraf i curs baix del riu Llobregat. Treb Mus Geol Barc. 16: 5–38.
- Devillard S, Aubineau J, Berger F, Marchandeu S. 2008. Home range of the European rabbit (*Oryctolagus cuniculus*) in three contrasting french populations. Mammalian Biology 73: 128–137.
- Estévez J. 1979. La fauna del Pleistoceno catalán. Unpublished PhD. Barcelona: Universitat de Barcelona.
- Ferro A, Juderías J.C., Nebot M., Pauné F. 1997. Sobre el hallazgo de *Lynx pardina* (Termminck) y otros vertebrados en el Avenc del Marge del Moro (Vallirana, Baix Llobregat). In: Federació Catalana d'Espeleologia editors. 7º Congreso Español de Espeleologia, Sant Esteve Sesrovires, 5–8 de diciembre 1997: Actes. Barcelona.
- Ferro A, Juderías JC, Nebot M, Pauné F. 1998. L'Avenc del Marge del Moro i altres cavitats, al Baix Llobregat. EspeleoSie 33: 92–98.

Fosse P, Fourvel JB, Madelaine S. 2020. Le *Lynx pardinus spelaeus* Boule, 1910 du Pleistocene moyen de la grotte de l'Escale (Bouches-du-Rhône, France): données paléontologiques et taphonomiques. *Paleo* 30: 108–137.

García-Perea R. 1996. Patterns of Postnatal Development in Skulls of Lynxes. Genus *Lynx* (Mammalia: Carnivora). *Jour Morph.* 229: 241–254.

García-Perea R, Gisbert J., Palacios F. 1985. Review of the Biometrical and Morphological Features of the Skull of the Iberian Lynx, *Lynx pardina* (Temminck, 1824). *Säuget Mitteil.* 32: 249–259.

Ghezzi E, Boscaini A, Madurell-Malapeira J, Rook L, 2015. Lynx remains from the pleistocene of Valdemino cave (Savona, northwestern Italy), and the oldest occurrence of *Lynx spelaeus* (carnivora, felidae). *Rend Linc.* 26: 87–95.

Ginsburg L. 1998. Le gisement de vertébrés pliocènes de Çalta, 5. Carnivores. *Geodiversitas* 20: 379–396.

Guzmán JN, García F.J, Garrote G, Pérez de Ayala R, Iglesias C. 2004. El lince ibérico (*Lynx pardinus*) en España y Portugal. Censo diagnóstico de sus poblaciones. Madrid: Dirección General para la Biodiversidad.

Huynh HM, Khidas K, Bull R, McAlpine D.F. 2019. Morphological and craniodental characterization of Bobcat × Canada Lynx (*Lynx rufus* × *L. canadensis*) F1 hybrids from New Brunswick, Canada. *Special Publications, Museum of Texas Tech University*: 427–440.

Kurtén B. 1957. The bears and hyaenas of the interglacials. *Quaternaria* 4:69–81.

Kurtén B. 1978. The lynx from Etouaries, *Lynx issiodorensis* (Croizet & Jobert), Late Pliocene. *Ann Zool Fennici.* 15: 314–322.

Kurtén B, Granqvist E. 1987. Fossil pardel lynx (*Lynx pardina spelaea* Boule) from a cave in southern France. *Ann Zoo Fennici*. 24: 39–43.

Johnson WE, Godoy JA, Palomares F, Delibes M, Fernandes M, Revilla E, O'Brien S. 2004. Phylogenetic and Phylogeographic Analysis of Iberian Lynx Populations. *Jour Hered*. 95: 19–28.

Li G, Davis BW, Eizirik E, Murphy WJ. 2016. Phylogenomic evidence for ancient hybridization in the genomes of living cats (Felidae). *Gen Resear*. 26: 1–11.

Mecozzi B, Sardella R, Boscaini A, Cherin M, Costeur L, Madurell-Malapeira J, Pavia M, Profico A, Iurino D. A. 2021. The tale of a short-tailed cat: New outstanding Late Pleistocene fossils of *Lynx pardinus* from southern Italy. *Quat Sci Revi*.
<https://doi.org/10.1016/j.quascirev.2021.106840>.

Palombo M. R, Sardella R, Novelli M. 2008. Carnivora dispersal in Western Mediterranean during the last 2.6 Ma. *Quaternary International* 179: 176–189.

Alejandro R, Calzada J. 2015. *Lynx pardinus* (errata version published in 2020). The IUCN Red List of Threatened Species 2015. e.T12520A174111773.

Rodríguez R, Ramírez O, Valdiosera C.E, García N, Alda F, Madurell-Malapeira J, Marmi J, Doadrio I, Willerslev E, Götherström A, Arsuaga J.L, Thomas MG, Lalueza-Fox C, Dalén L. 2011. 50,000 years of genetic uniformity in the critically endangered Iberian lynx. *Mol ecol*. 20: 3785–3795.

Rodríguez-Hidalgo A, Sanz M, Daura J, Sánchez-Marco A. 2020. Taphonomic criteria for identifying Iberian lynx dens in quaternary deposits. *Scientific reports*.

https://doi.org/10.1038/s41598-020-63908-6_1

Rodríguez-Varela V, Tagliacozzo A, Ureña I, García N, Crégut-Bonnoure E, Mannino MA, Arsuaga JL, Valdiosera C. 2015. Ancient DNA evidence of Iberian Lynx palaeoendemism. *Quat Sci Review* 11:172–180.

Rovinsky D. 2020a. Media 000115967. Element unspecified [Mesh] [Strlig]. Morphosource; [accessed 2020 May 10].
<https://www.morphosource.org/concern/media/000115967?locale=en>

Rovinsky D. 2020b. Media 000115454. Element unspecified [Mesh] [Strlig]. Morphosource; [accessed 2020 May 10]
<https://www.morphosource.org/concern/media/000115454?locale=en>

Rovinsky D. 2020c. Media 000115455. Element unspecified [Mesh] [Strlig]. Morphosource; [accessed 2020 May 10]
<https://www.morphosource.org/concern/media/000115455?locale=en>

Santillini F, Bagliacca M. 2010. Habitat use by the european wild rabbit (*Oryctolagus cuniculus*) in a coastal sandy dune ecosystem of central Italy. *Hystrix* 21:4486.

Sarrión I. 1978. Un lince de las cavernas en la cueva del Puerto (Calasparra-Murcia). *Lapiaz* 2: 7–26.

Simón M.A. 2013. Censo de las poblaciones andaluzas de lince ibérico, año 2012. Life+Iberlince website; [accessed 14 Nov 2021]. www.iberlince.eu.

Testu A. 2006. Etude paléontologique et biostratigraphique des Felidae et Hyenidae pléistocène de l'Europe méditerranéenne. Unpublished PhD. Perpignan: Université de Perpignan.

Viret J. 1954. Le loess à bancs durcis de Saint-Vallier (Drôme) et sa faune de mammifères villafranchiens. *Nouv Arch Mus Hist Nat.* 4: 1–200.

Von den Driesch A. 1976. A guide to the measurement of animal bones from archaeological sites: as developed by the Institut für Palaeoanatomie, Domestikationsforschung und Geschichte der Tiermedizin of the University of Munich (Vol. 1). Cambridge: Peabody Museum Press.

Werdelin L. 1981. The evolution of lynxes. *Ann. Zool. Fenn* 18: 37–71.

Wilson D. E, DeeAnn M. Reeder. 2005. *Mammal species of the world: A Taxonomic and Geographic Reference*. Baltimore: The Johns Hopkins University Press.

Witmer L. 2019.: Media 000067570. 3D Surface Image of Cranium Stl [Mesh][Etc]. Morphosource; [accessed 2020 May 10].

<https://www.morphosource.org/concern/media/000067570?locale=en>

Figure Captions

Figure 1. Avenc del Marge del Moro geographical location and structure. **A**, Cross-section: The letters indicate the recollection points where *Lynx pardinus* remains were found. Modified from Ferro et al. (1997). **B**, Location map of the site in the surroundings of the city of Barcelona.

Figure 2. *Lynx pardinus* 3D model of the cranium IPS 4175 from Avenc del Marge del Moro.

Figure 3. *Lynx pardinus* 3D model of the cranium IPS 4176 from Avenc del Marge del Moro.

Figure 4. *Lynx pardinus* postcranial remains from Avenc del Marge del Moro. **A**, IPS 4215, right humerus distal epiphysis. A1: caudal view; A2: cranial view; A3: lateral view; A4: medial view. **B**, IPS 4233, right scapula. B1: dorsal view; B2: ventral view. **C**, IPS 4201, left humerus distal fragment. C1: caudal view; C2: cranial view; C3: lateral view; C4 medial view. **D**, IPS 4198, right radius proximal fragment. D1: caudal view; D2 cranial view; D3:

lateral view; D4: medial view. **E**, IPS 4244, left scapula. E1: dorsal view; E2: ventral view. **F**, IPS 4218, left Mtc III. F1: dorsal view; F2: palmar view; F3: lateral view; F4: medial view; F5: proximal view. **G**, IPS 4197, left radius' proximal fragment. G1 caudal view; G2: cranial view; G3: lateral view; G4: medial view. **H**, IPS 4202: left ulna with distal epiphysis not preserved. H1 caudal view; H2: cranial view; H3: lateral view; H4: medial view.

Figure 5. *Lynx pardinus* postcranial remains from Avenc del Marge del Moro. **A**, IPS 4220, left Mtt V. A1: palmar view; A2: dorsal view; A3: lateral view; A4: medial view; A5: proximal view. **B**, IPS 4217, left Mtt IV. B1: palmar view; B2: dorsal view; B3: lateral view; B4: medial view; B5: proximal view. **C**, IPS 4216, left Mtt III. C1: palmar view; C2: dorsal view; C3: lateral view; C4: medial view; C5: proximal view. **D**, IPS 4219, left Mtt II. D1: palmar view; D2: dorsal view; D3: lateral view; D4: medial view; D5: proximal view. **E**, IPS 4213, right tibia. E1: caudal view; E2: cranial view; E3: lateral view; E4: medial view. **F**, IPS 4212, left tibia. F1: caudal view; F2: cranial view; F3: lateral view; F4: medial view. **G**, IPS 4211, left hemipelvis. G1: cranio-lateral view; G2: medio-caudal view. **H**, IPS 4214, left femur. H1: caudal view; H2: cranial view; H3: lateral view; H4: medial view.

Figure 6. Basicranial shape comparison between different *Lynx* species. **A**, *Lynx pardinus* from Avenc del Marge del Moro (IPS 4175); **B**, *Lynx pardinus* from Avenc del Marge del Moro (IPS 4176). **C**, *Lynx pardinus* from Ingarano MGPT-PU 135415); **D**, *Lynx pardinus* from Avenc Marcel (IPS 4170); **E**, *Lynx pardinus* from Grotte de l'Observatoire, modified from Boule and Villeneuve (1927); **F**, extant *Lynx pardinus* (IPS 82320); **G**, extant *Lynx rufus*; **H**, extant *Lynx rufus*; **I**, extant *Lynx canadensis*; **J**, extant *Lynx canadensis* (IPS 82318); **K**, extant *Lynx rufus* (IPS 82317); **L**, *Lynx issiodorensis* from Saint-Vallier (MNB StV.767); **M**, extant *Lynx lynx*; **N**, extant *Lynx lynx*; **O**, *Lynx issiodorensis*

from Olivola (MNB Ol 1); **P**, *Lynx issiodorensis* from Pantalla(SABAP_UMB 337653); **Q**, extant *Lynx lynx* (MZB2010-1402); **R**, extant *Lynx lynx*, modified from Rovinsky (2020c).

Figure 7. Boxplots of the mesiodistal length of the fourth upper premolar in different *Lynx* species grouped following geographical and chronological criteria.

	IPS 4175	IPS 4176
Total length	123.2	-
Condylbasal length	115.5	-
Basal length	104.8	-
Length of the sagittal crest	15.9	21.4
Distance between the lineae temporalis	28.46	15.96
Length of the temporalis ridges	-	52.3
Zygomatic breadth	-	-
Greatest neurocranium breadth	56.7	58.4
Breadth of the postorbital constriction	45.2	42.2
Greatest mastoid breadth	55.3	60

Table 1. Cranial measurements (mm) of *Lynx pardinus* from Avenc del Marge del Moro.

Catalog no.	Side	C			P3		P4					
		L	W	H	L	W	L	W	Lpr	Lps	Lpa	Lms
Upper dentition												
IPS 4242	left	8.1	6.2	-								
IPS 4178	left				11.2	5.6	16.3	8.5	3.9	3.2	7.3	6.6
IPS 4177	left				11.5	5.4	16.8	8.5	3.6	2.9	6.6	7.2
IPS 4175	right				10.4	5.2	15.7	7.7	3.3	4	6.5	7.1
IPS 4175	left				10.3	5.2	16.4	7.8	3.8	3.6	6.5	6.9
IPS 4181	left				10.8	5.3						
IPS 4179	left						17.6	7.7	3.76	3.56	7.2	7.1
Lower dentition												
IPS 4221	right	7.7	6.3	17.7								
IPS 4222	right	7.5	6.3	16								
IPS 4180	right						10.7	5.26				
IPS 4241	-	7.7	6.3	18								

Table 2. Dental measurements (mm) of *Lynx pardinus* from Avenc del Marge del

Moro.

Catalog no.	Side	GL	DT prox.	DAP prox.	DT dist.	DAP dist.	DT diaf.	DAP diaf.
Humerus								
IPS 4201	left	-	-	-	29.3	18.2	-	-
IPS 4215	right	-	-	-	-	16.8	-	-
Radius								
IPS 4198	right	-	13.4	9.1	-	-	9.4	5.8
IPS 4193	right	-	14.5	10.7	-	-	-	-
IPS 4197	left	-	14.3	10.4	-	-	-	-
Ulna								
IPS 4202	left	-	9.7	15.9	-	-	6.2	11.9
Femur								
IPS 4214	left	-	-	-	29.7	19.2	-	-
Tibia								
IPS 4212	left	-	-	-	22.5	16.2	10.2	12.4
IPS 4213	right	-	-	-	22.6	15	11.5	14.1
II Metatarsus								
IPS 4194	right	75.6	6.5	11.5	8.9	8.9	6.4	5.7
IPS 4219	left	75.5	6.5	11.4	9	8.8	5.9	5.5
IPS 4250	right	-	6	11.2	-	-	6	5.1
III Metatarsus								
IPS 4216	right	80.3	11.2	14.46	10.5	9.6	8	5
IPS 4199	left	-	10	15.5	-	-	8.6	6.2
IPS 4204	right	-	11.3	16	-	-	-	-
IV Metatarsus								
IPS 4200	right	-	-	11.5	-	-	-	-
IPS 4217	left	-	7.5	11.9	-	-	-	-
V Metatarsus								
IPS 4220	left	74.4	9.1	5.7	8	8.2	3.9	4.4
IPS 4195	left	-	11.2	6.3	-	-	-	-
III Metacarpus								
IPS 4218	right	56.9	8.4	9.7	8.7	7.7	4.8	4.5
I Phalanx								
IPS 4192		31.2	9.4	5.9	7.4	5.8	6.4	4.2
IPS 4186		16.6	5.7	4.4	4.4	3.7	3.8	2.9
IPS 4187		28.3	8.5	6.4	6.7	6.4	5.3	3.6
IPS 4186		27.6	8.8	7.5	7	5.5	6.1	4.2
IPS 4191		25.2	8.5	7.5	7.3	5.5	5.7	4.8
IPS 4184		21.3	7.2	7.2	6	4.5	4.8	4.4
IPS 4188		26.8	8.1	6.5	6.2	4.7	4.8	3.6
IPS 4189		23.9	8.1	6.8	6.3	5.2	5.3	4.2
IPS 4190		21.2	7.6	5.86	5.8	4.8	4.6	4.2

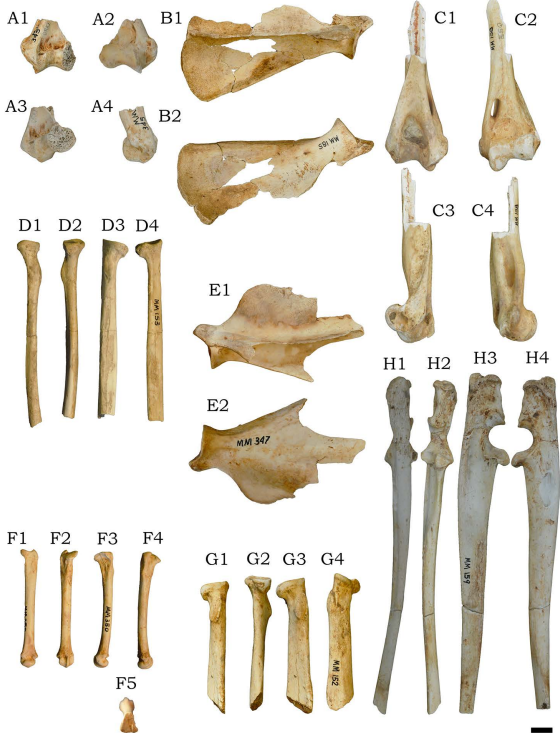
Table 3. Long bones' measurements (mm) of *Lynx pardinus* from Avenc del Marge del Moro.

Catalog no.	Side	HS	SLC	GLP	LG	BG	
Scapula							
IPS 4232	left	-	21.1	24.3	22.7	16.3	
IPS 4243	left	-	20.1	24.3	22.7	16.3	
IPS 4244	left	-	17.2	21.7	20	15.4	
IPS 4233	right	92.1	-	21.7	21.2	14.8	
IPS 4231	right	-	21	24.4	22.4	16.6	
		GL	LA	SH	SB	Lfo	
Pelvis							
IPS 4211	left	-	17.7	20	6.7	31.8	
IPS 4210	left	-	17.6	18.5	5	30.5	
		HFcr	BFcr	Bpacr	Bpacd	H	PL
Lumbar vertebrae							
IPS 4240		6.1	11.2	-	8.5	17.4	17
IPS 4239		7.4	9.26	-	-	-	-
IPS 4245		-	-	-	12.7	-	-
IPS 4234		14	19.9	22.1	14.9	42.7	34
IPS 4235		13.3	18.5	20.2	13.8	-	33.5
IPS 4236		15.7	22	-	-	-	27.7
Cervical vertebrae							
IPS 4223		6.7	11.6	-	-	-	16.9

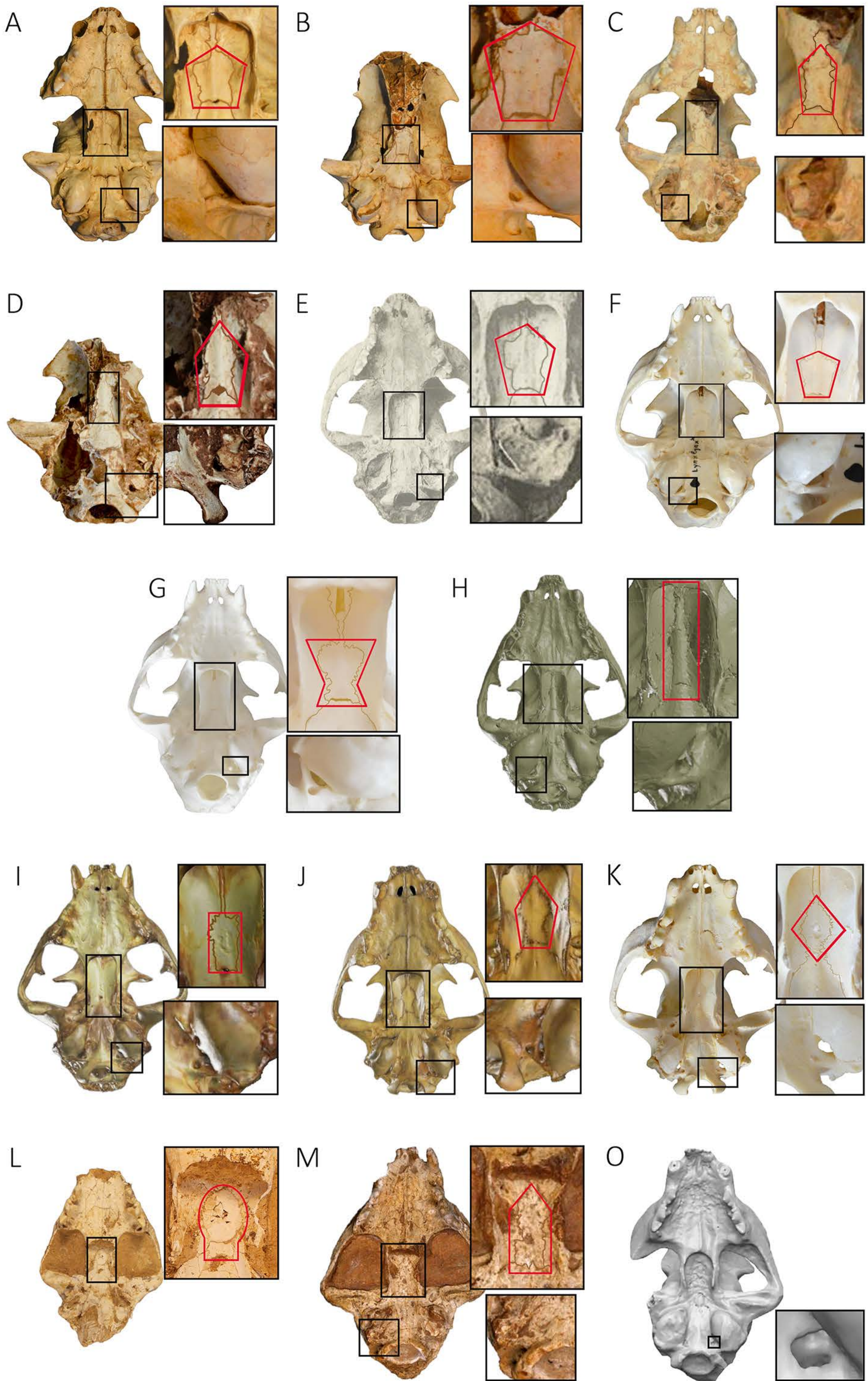
Table 4. Vertebrae, scapula and pelvis measurements (mm) of *Lynx pardinus* from Avenc del Marge del Moro.

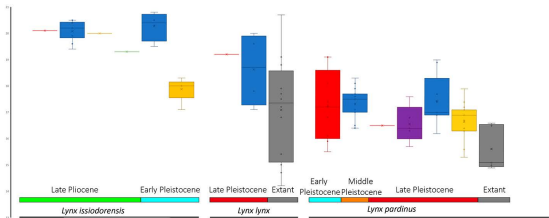
Species	Location	Age		Humerus		Radius				Ulna				
				DT dist.	DAP dist.	DT prox.	DAP prox.	DT diaf.	DAP diaf.	DT prox.	DAP prox.	DT diaf.	DAP diaf.	
<i>Lynx pardinus</i>	Avenc del Marge del Moro	Late Pleistocene	N	1	2	3	3	1	1	1	1	1	1	
			X	29.30	17.50	14.07	10.70	9.40	5.80	9.70	15.90	6.20	11.90	
			Min.		16.80	13.40	9.10							
			Max.		18.20	14.50	10.70							
			SD		0.70	0.48	0.69							
<i>Lynx lynx</i>	France	Late Pleistocene	N	1	1			1	1	1	1	1	1	
			X	39.20	21.40			11.30	7.50	13.10	18.60	7.70	13.30	
			Min.											
			Max.											
			SD											
<i>Lynx lynx</i>	Iberian Peninsula	Late Pleistocene	N	1	1									
			X	40.50										
			Min.											
			Max.											
			SD											
<i>Lynx lynx</i>		Extant	N	8	7	5	4	5	4	3	3	3	3	
			X	37.08	21.43	14.66	13.55	11.82	5.95	11.57	18.30	7.43	12.57	
			Min.	27.30	16.20	11.90	10.50	8.80	4.30	10.40	17.90	7.20	11.90	
			Max.	40.90	24.20	16.80	15.90	13.20	6.90	13.10	18.60	7.70	13.30	
			SD	4.10	2.48	1.70	1.95	1.61	0.99	1.13	0.29	0.21	0.57	
<i>Lynx pardinus</i>	France	Middle Pleistocene	N	5	1	5	1	5	5			1	1	
			X	31.92	17.70	13.94	12.10	10.84	6.12			6.00	10.5	
			Min.	29.10		12.70		9.70	5.40					
			Max.	36.90		15.30		12.00	7.00					
			SD	2.74		0.99		0.87	0.56					
<i>Lynx pardinus</i>	France	Late Pleistocene	N	9	9	5	5	4	4	3	2	2	2	
			X	32.79	19.56	14.78	12.12	11.48	6.43	12.10	18.50	6.85	14.45	
			Min.	28.10	18.30	14.10	11.5	11.00	6.20	10.20	17.00	6.40	14.30	
			Max.	38.30	21.60	15.40	13.2	12.10	6.70	13.30	20.00	7.30	14.60	
			SD	2.76	1.08	0.44	0.64	0.49	0.19	1.36	1.50	0.45	0.15	
<i>Lynx pardinus</i>		Extant	N	2	1	4	2	3	2	1	1	1	1	
			X	27.50	16.30	12.90	10.9	9.23	5.25	8.30	15.10	6.30	12.20	
			Min.	27.50		12.00	10.6	8.90	5.00					
			Max.	27.50		13.69	11.2	9.80	5.5					
			SD	0.00		0.63	0.3	0.40	0.25					

Table 5. Anterior limb bones comparison between Avenc del Marge del Moro *Lynx pardinus*. and *Lynx Lynx* and *Lynx pardinus*. (N: Number of remains; X: Average; Min.: minimum measurement; Max.: maximum measurement; SD: Standard deviation).









■ Iberian peninsula
 ■ France
 ■ Italy
 ■ Turkey
 ■ Extant
 ■ Avenc del Marge del Moro

1

A1



A2



A4



A3

**2**

B1



B2



B4



B3



C1



C2



C3



D1



D2



D3



A1



A2



B1



B2



C1



C2



A3



B3



C3



D1



D2



E1



E2



F1



F2



G1



G2

